the device ground plane functions more like a radiator in the lower band and more like a reflector in the higher band, especially in the high-frequency portion of the higher band.

4. CONCLUSION

A very-low-profile dual-wideband tablet device antenna for the LTE/WWAN operation in the 698–960 and 1710–2690-MHz bands has been proposed and studied. The antenna includes a driven strip and a shorted parasitic strip, and both are configured such that proper coupling therebetween can be obtained which leads to wideband resonant modes thereof excited. Also, it has been shown that with the aid of a high-pass matching circuit integrated therein, significant bandwidth enhancement in the antenna's lower band can be obtained. Hence, with the proposed design, the antenna can provide two wide operating bands to cover the whole band of the LTE/WWAN operation with a very low profile of 8 mm and a small occupied volume of $3.8 \times 8 \times 50$ mm^3. The proposed antenna is promising for practical applications in modern tablet computers that are with narrow spacing between the display panel and device frame thereof.

REFERENCES

1. K.L. Wong and M.T. Chen, Small-size LTE/WWAN printed loop antenna with an inductively coupled branch strip for bandwidth enhancement in the tablet computer, IEEE Trans Antennas Propag 61 (2013), 6144–6151.
2. K.L. Wong and T.W. Weng, Small-size triple-wideband LTE/WWAN tablet device antenna, IEEE Antennas Wireless Propag Lett 12 (2013), 1516–1519.
3. W.S. Chen and W.C. Jhang, A planar WWAN/LTE antenna for portable devices, IEEE Antennas Wireless Propag 12 (2013), 19–22.
4. Y.L. Ban, S.C. Sun, J.L.W. Li, and W. Hu, Compact coupled-fed wideband antenna for internal eight-band LTE/WWAN tablet computer applications, J Electromagn Waves Appl 26 (2012), 2222–2233.
5. S.H. Chang and W.J. Liao, A broadband LTE/WWAN antenna design for tablet PC, IEEE Trans Antennas Propag 60 (2012), 4354–4359.
6. K.L. Wong and T.J. Wu, Small-size LTE/WWAN coupled-fed loop antenna with band-stop matching circuit for tablet computer, Microwave Opt Technol Lett 54 (2012), 1189–1193.
7. J.H. Lu and Y.S. Wang, Internal uniplanar antenna for LTE/GSM/UMTS operation in a tablet computer, IEEE Trans Antennas Propag 61 (2013), 2841–2846.
8. J.H. Lu and F.C. Tsai, Planar internal LTE/WWAN monopole antenna for tablet computer application, IEEE Trans Antennas Propag 61 (2013), 4358–4363.
9. K.L. Wong, H.J. Jiang, and T.W. Weng, Small-size planar LTE/WWAN antenna and antenna array formed by the same for tablet computer application, Microwave Opt Technol Lett 55 (2013), 1928–1934.
10. K.L. Wong and W.J. Lin, WWAN/LTE printed slot antenna for tablet computer application, Microwave Opt Technol Lett 54 (2012), 44–49.
11. M. Tzortzakakis and R.J. Langley, Quad-band internal mobile phone antenna, IEEE Trans Antennas Propag 55 (2007), 2097–2103.
12. Z. Zhang, J.C. Langer, K. Li, and M.F. Iskander, Design of ultrawideband mobile phone stubby antenna (824 MHz-6 GHz), IEEE Trans Antennas Propag 56 (2008), 2107–2111.
13. K.L. Wong and T.W. Kang, GSM850/900/1800/1900/UMTS printed monopole antenna for mobile phone application, Microwave Opt Technol Lett 50 (2008), 3192–3198.
14. S. Jeon, Y. Liu, S. Ju, and H. Kim, PIFA with parallel resonance feed structure for wideband operation, Electron Lett 47 (2011), 1263–1265.
15. K.L. Wong, Y.W. Chang, and S.C. Chen, Bandwidth enhancement of small-size WWAN tablet computer antenna using a parallel-resonant spiral slit, IEEE Trans Antennas Propag 60 (2012), 1705–1711.
16. K.L. Wong, T.J. Wu, and P.W. Lin, Small-size uniplanar WWAN tablet computer antenna using a parallel-resonant strip for bandwidth enhancement, IEEE Trans Antennas Propag 61 (2013), 492–496.
17. K.L. Wong and W.J. Lin, WWAN printed monopole slot antenna with a parallel-resonant slit for tablet computer application, Microwave Opt Technol Lett 55 (2013), 40–45.
18. S. Jeon and H. Kim, Mobile terminal antenna using a planar inverted-E feed structure for enhanced impedance bandwidth, Microwave Opt Technol Lett 54 (2012), 2133–2138.
19. K.L. Wong and T.J. Wu, Small planar internal WWAN tablet computer antenna, Microwave Opt Technol Lett 54 (2012), 426–431.
20. Z. Chen, Y. Ban, S. Sun, and J.L.W. Li, Printed antenna for penta-band WWAN tablet computer application using embedded parallel resonant structure, Prog Electromagn Res 136 (2013), 725–737.
21. ANSYS HFSS. Available at: http://www.ansys.com/products/hf/hfss/.
22. Z. Li and Y. Rahmat-Samii, Optimization of PIFA-IFA combination in handset antenna designs, IEEE Trans Antennas Propag 53 (2005), 1770–1778.

A PLANAR RECONFIGURABLE ANTENNA WITH BIDIRECTIONAL END-FIRE AND BROADSIDE RADIATION PATTERNS

Longsheng Liu, Wendong Liu, Yue Li, Zhijun Zhang, and Zhenghe Feng
Department of Electronic Engineering, State Key Lab of Microwave and Communications, Tsinghua University, Beijing 100084, China; Corresponding author: zjzh@tsinghua.edu.cn

Received 8 December 2013

ABSTRACT: *The design of a planar reconfigurable antenna with bidirectional end-fire and broadside radiation patterns from a common aperture is presented in this article. The proposed antenna is composed of two series-feed collinear slot subarrays corporately fed by a microstrip line and two series-feed dipole subarrays corporately fed by a microstrip line-to-double side parallel strip line transition, respectively. A prototype for 2.4 GHz wireless local area networks applications is fabricated and measured. The measured realized gains are about 11—12 and 7–8 dBi for broadside and end-fire patterns. Experimental results, which agree with the simulated ones, verify that the proposed antenna is a good candidate for pattern reconfigurable applications.* © 2014 Wiley Periodicals, Inc. Microwave Opt Technol Lett 56:1942–1946, 2014; View this article online at wileyonlinelibrary.com. DOI 10.1002/mop.28486

Key words: *pattern reconfigurable; bidirectional; end-fire; broadside; collinear slot array*

1. INTRODUCTION

With the rapid development of wireless communication, pattern reconfigurable antennas have drawn lots of attention because they enable to provide dynamic radiation coverage, mitigate multipath fading, and improve beam steering capability of phased array systems. In the past decades, there exists an extensive literature on the design of pattern reconfigurable antennas [1–9]. Different methods are used to reconfigure the radiation pattern: one way is selection of different radiating structure including shorting sections [1], parasitic elements [2,3], and antenna shape [4], or adjustment of radiating elements [5,6], another is switching between different feed networks [7–9].

In this article, a two-port pattern diversity antenna providing bidirectional end-fire and broadside radiation patterns from a

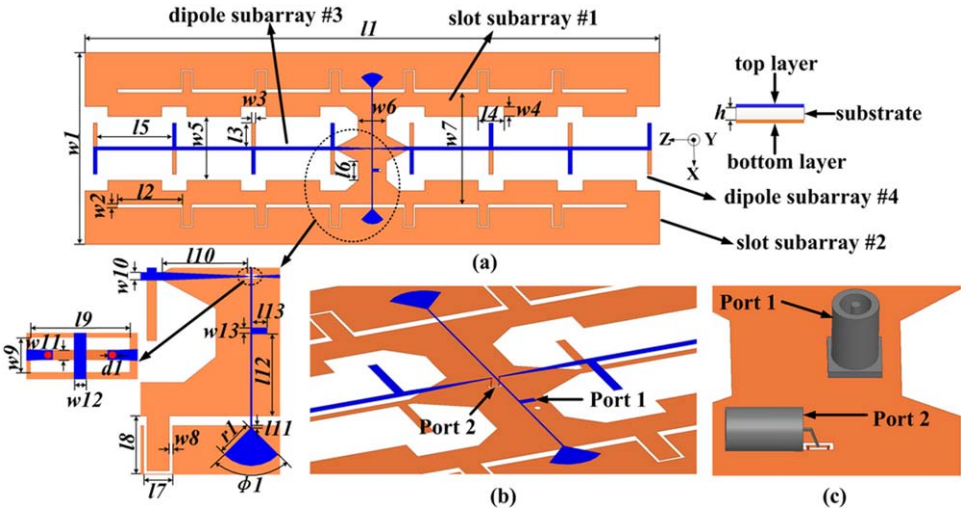

Figure 1 Geometry of the proposed antenna (a) top view, (b) 3D view of the feed structures including the crossover, and (c) 3D view of the feed ports. [Color figure can be viewed in the online issue, which is available at wileyonlinelibrary.com]

common aperture has been presented. The proposed antenna has the capacity of reconfiguring radiation pattern from a planar, low profile, and symmetric structure, which could be used in the places where bidirectional communication is needed such as coal mine, tunnel, bridge, railway, or crossroads.

This article is organized as follows, the proposed structure and operation mechanism will be introduced in Section 2, in Section 3, the simulated and experimental results will be shown, and some conclusion will be drawn in the end.

2. ANTENNA DESIGN

2.1. Antenna Structure

Figure 1 shows the geometry of the proposed two-port pattern reconfigurable antenna with broadside and end-fire radiation patterns for bidirectional communication applications. The proposed antenna is designed on a double-sided metalized FR4_epoxy dielectric substrate with a relative permittivity of 4.6, loss tangent of 0.02, and overall size of 450 × 150 × 1 mm^3. It has a planar, low profile, and symmetric configuration, consisting of two series-feed collinear slot subarrays [10] corporately fed by a microstrip line and two series-feed dipole subarrays corporately fed by a microstrip line-to-double side parallel strip line (MS-to-DSPSL) transition, respectively. As shown in Figures 1(a) and 1(b), a crossover is used to realize the orthogonal configuration of the two feed structures, which is beneficial to improve the isolation between the two ports. The antenna is simulated with the aid of ANSYS HFSS and the optimal values of the parameters labeled in Figure 1 are provided in Table 1.

The evolution of the proposed antenna is shown in Figure 2. As shown in Figures 2(a) and 2(b), at first, a bidirectional broadside antenna composed of two series-feed collinear slot subarrays is designed; and then, the ground is modified into a dumbbell-shaped defected ground structures (DGS), therefore, the dipole array illustrated in Figure 2(c) can be easily inserted into two rectangular defected areas without increasing the size of the proposed structure. The distance between the two slot subarrays is $w_2 + w_7 = 90$ mm (about 0.73 free space wavelength at 2.45 GHz) to reach a compromise between the gain of the slot array and space left for inserting the dipole array. The dipole array, illustrated in Figure 2(c), consisting of two series-feed dipole subarrays corporately fed by a MS-to-DSPSL transition is initially designed for end-fire pattern while the influence of the dumbbell-shaped DGS on performance of the dipole array is taken into consideration in Figure 2(d). A pattern reconfigurable antenna shown in Figure 2(e) is formed by combing the structures in Figures 2(b) and 2(d). To increase the gain of the dipole array and the isolation between two feed ports on the premise that the impact on the performance of the slot array is as small as possible, the proposed antenna finally evolves into Figure 2(f).

2.2. Operation Mechanism

It is well known that an array with an in-phase excitation has a broadside radiation pattern. By changing the excitation to the alternative out-of-phase and keeping the distance between adjacent elements at half wavelength, an end-fire pattern is obtained.

Based on the one fed by a coplanar waveguide in [10], series-feed collinear slot subarrays #1 and #2 are corporately fed by microstrip line in this article. When port 1 is excited, all the horizontal end-to-end slotlines of $l_2 \times w_2$ behave as the radiators, whereas the meandered slotlines of $(l7 + 2 \times l8) \times w8$ serve as the feeding network. Both the radiating slotline and meandered slotline sections are approximately a half guided-wavelength of the slotline transmission line at 2.45 GHz; therefore, all the radiating slotlines are excited in phase for each subarray #1 and #2. To compensate for the out-of-phase excitations

TABLE 1 Dimensions of the Proposed Antenna

Parameters	l_1	l_2	l_3	l_4	l_5	l_6	l_7	l_8	l_9	l_{10}
Value	450	51	18.75	20	59	15	9	18	4	26.5
Parameters	L_{11}	l_{12}	l_{13}	w_1	w_2	w_3	w_4	w_5	w_6	w_7
Value	0.75	25.5	4.75	150	3	3	8	50	22	87
Parameters	w_8	w_9	w_{10}	w_{11}	w_{12}	w_{13}	d_1	r_1	h	Φ_1
Value	1	1.4	2.5	0.5	0.5	2	0.3	12	1	90

All the values are in millimeters except that Φ_1 in degree.

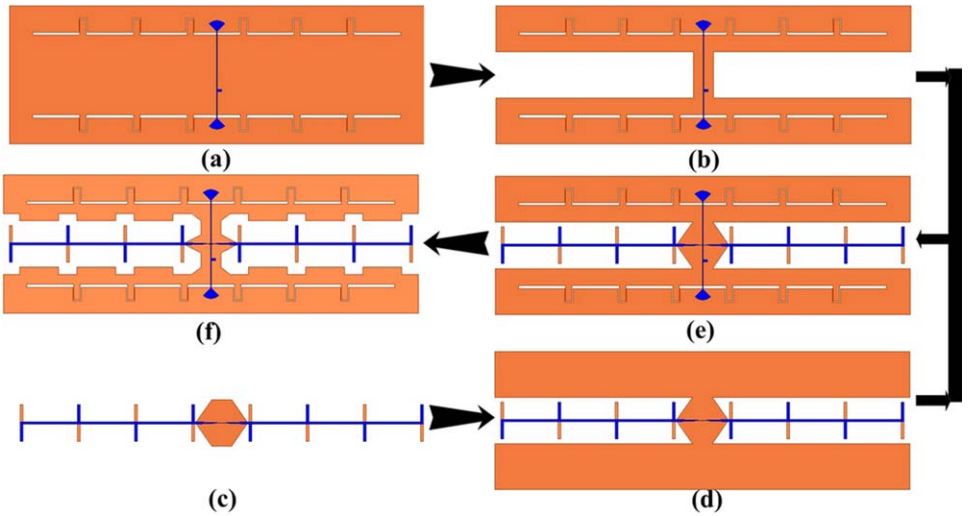

Figure 2 Evolution of the proposed antenna. [Color figure can be viewed in the online issue, which is available at wileyonlinelibrary.com]

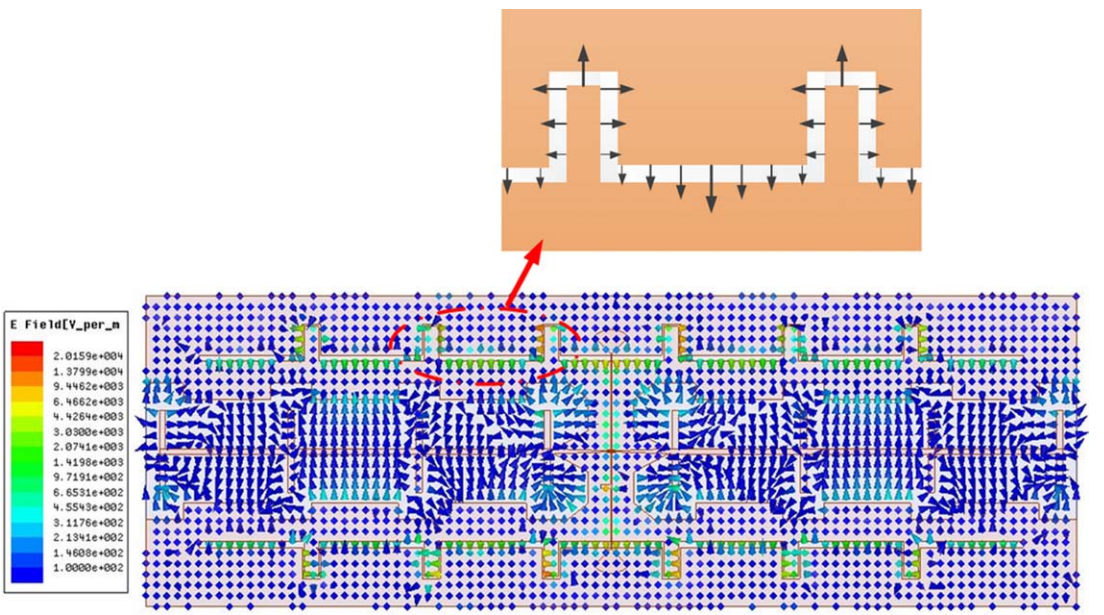

Figure 3 Instantaneous electric field distributions at 2.45 GHz for port 1. [Color figure can be viewed in the online issue, which is available at wileyonlinelibrary.com]

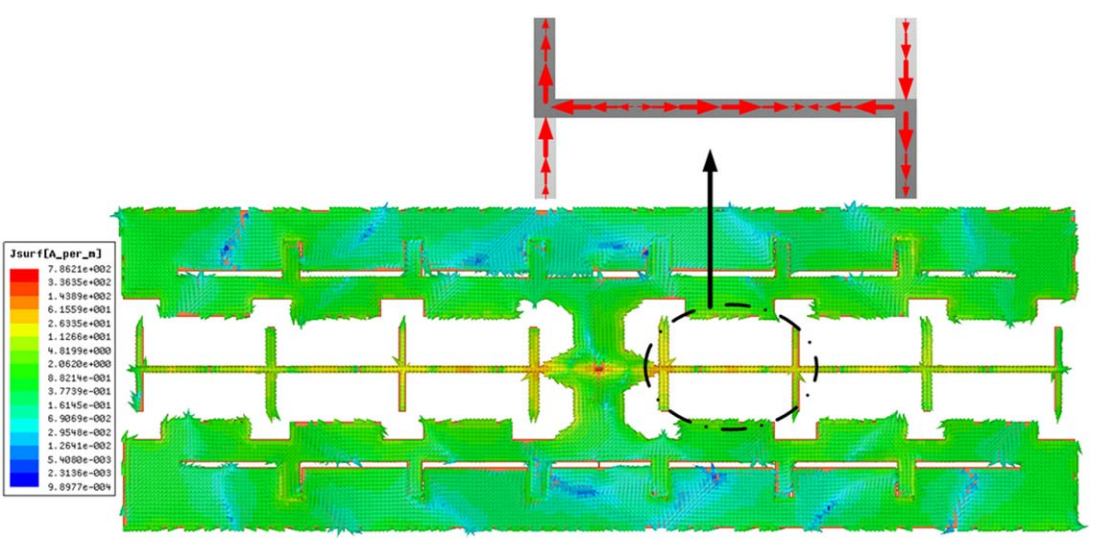

Figure 4 Instantaneous surface current distributions at 2.45 GHz for port 2. [Color figure can be viewed in the online issue, which is available at wileyonlinelibrary.com]

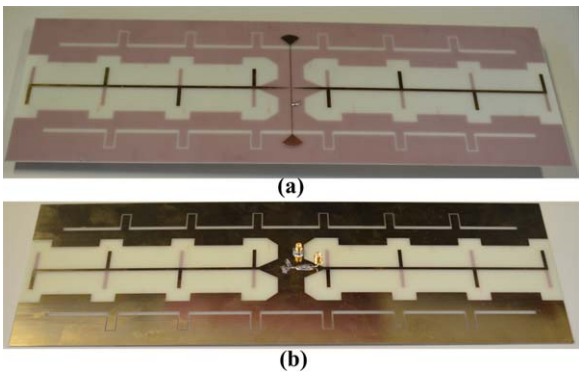

Figure 5 Photograph of the proposed antenna. [Color figure can be viewed in the online issue, which is available at wileyonlinelibrary.com]

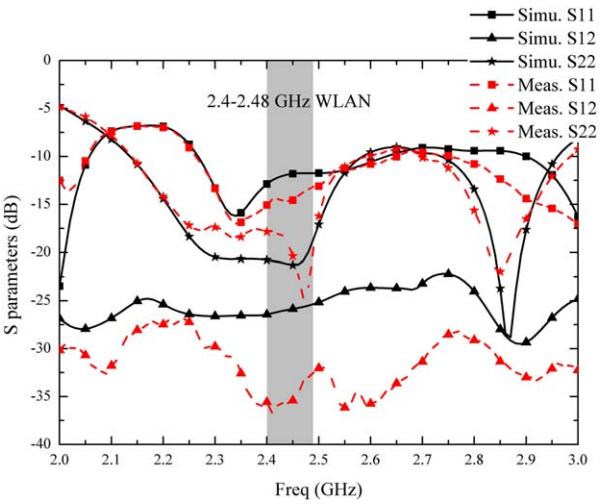

Figure 6 Simulated and measured *S*-parameters. [Color figure can be viewed in the online issue, which is available at wileyonlinelibrary.com]

from the microstrip line, the whole slot array is off-set fed by port 1 with another differential phase delay of about 180° to ensure the in-phase excitation of all the radiating elements and reinforce broadside radiation pattern. The electric field distributions on the apertures of the proposed antenna at 2.45 GHz are shown in Figure 3 where the directions and sizes of the arrows indicate the directions and magnitudes of the electric field, respectively.

DSPSLs are used to feed #3 and #4 in a relatively simple series configuration. The distance between adjacent elements is approximately one guided-wavelength; therefore, phase reversal technique is used to obtain out-of-phase current on every element. Moreover, a MS-to-DSPSL transition is utilized as a balun and impedance transformer. When port 2 is excited, the surface current distributions at 2.45 GHz are depicted in Figure 4.

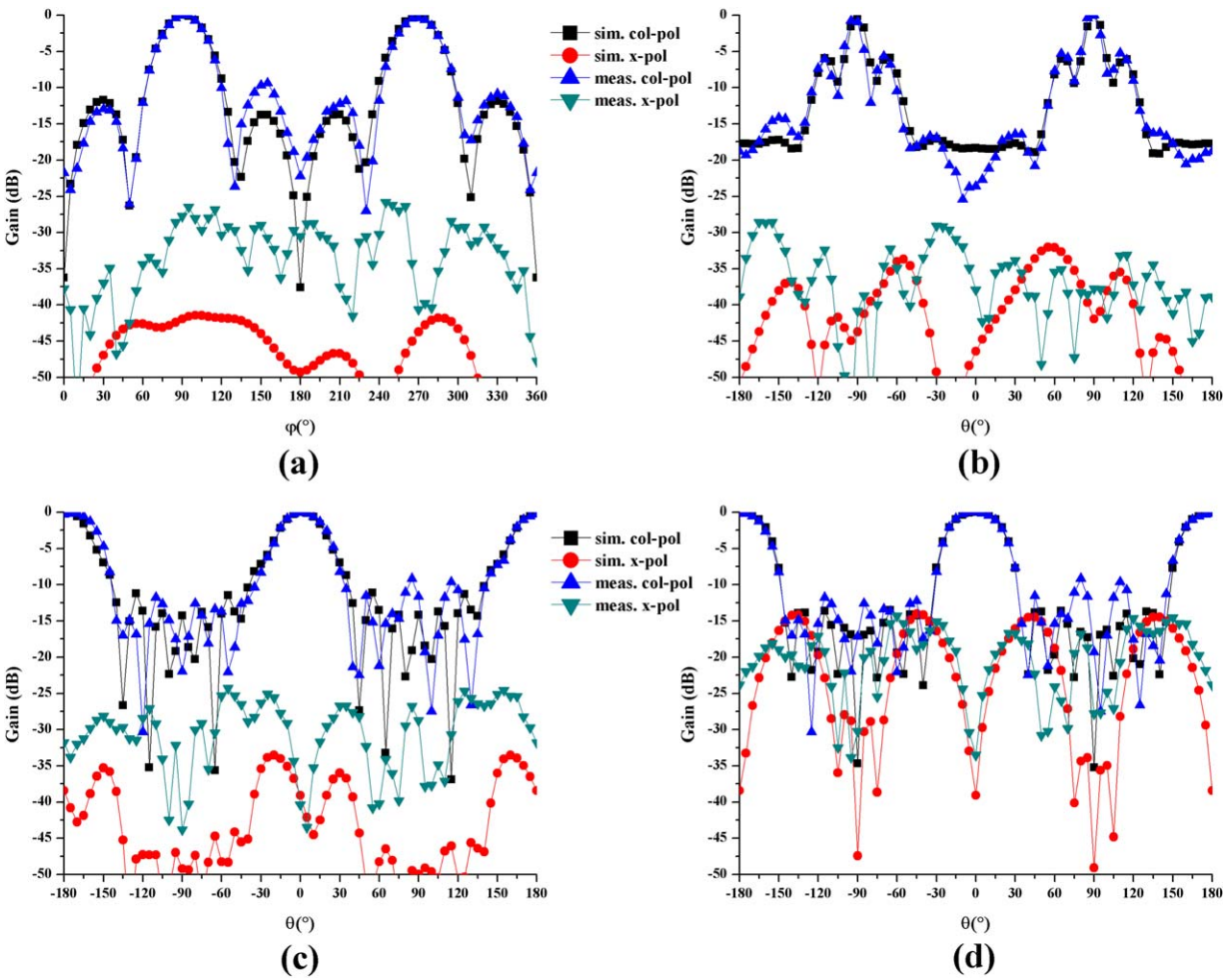

Figure 7 Simulated and measured normalized radiation patterns at 2.45 GHz. (a) *xy*-plane for port 1, (b) *yz*-plane for port 1, (c) *xz*-plane for port 2, and (d) *yz*-plane for port 2. [Color figure can be viewed in the online issue, which is available at wileyonlinelibrary.com]

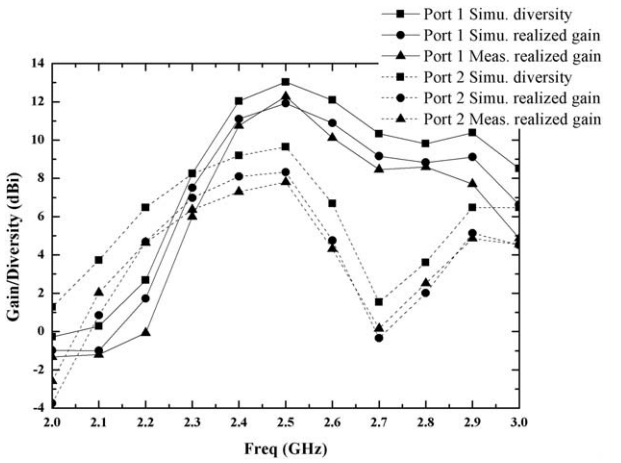

Figure 8 Simulated diversity, simulated realized gain, and measured realized gain against frequency

3. RESULTS AND DISCUSSION

To demonstrate the validity of the presented design strategy, as depicted in Figure 5, a prototype antenna was fabricated and measured. The reflection coefficients were obtained by a vector network analyzer Agilent ENA E5071B while the radiation patterns were measured in an ETS-Lindgren© anechoic chamber [11]. Simulated and measured results are given in Figures 6–8. Good agreement between them could be observed.

3.1. S-Parameters

Both the simulated and measured *S*-parameters are shown in Figure 6. The simulated and measured impedance bandwidths ($S_{11} \leq -10$ dB) are 2.27–2.63 GHz and 2.26–2.65 GHz for port 1 whereas the simulated and measured ones are 2.14–2.58 GHz and 2.14–2.60 GHz for port 2. The simulated isolation between the two ports is better than −25 dB whereas the measured result demonstrates isolation better than −30 dB.

3.2. Radiation Pattern

Figure 7 illustrates the simulated and measured normalized radiation patterns at 2.45 GHz.

For port 1, as shown in Figures 7(a) and 7(b), bidirectional broadside pattern is obtained with the main beam directing positive and negative *Y* in both *xy*- and *yz*-planes. The simulated and measured cross-polarization values are better than −40 and −25 dB.

From Figures 7(c) and 7(d), bidirectional end-fire pattern is obtained when port 2 is excited. The simulated and measured cross-polarization values are better than −35 and −20 dB.

3.3. Diversity and Realized Gain

Figure 8 depicts the simulated diversity, simulated realized gain, and measured realized gain of the proposed antenna against frequency. The diversity and gain are given at $\theta = 90°$, $\phi = 90°$ for port 1 and $\theta = 0°$, $\phi = 0°$ for port 2.

Over the 2.4 GHz wireless local area networks (WLAN) band, the simulated diversity is 12–13 dBi for port 1 whereas 9–10 dBi for port 2. Simulated realized gains are about 1 dB lower than diversity mainly owing to metal loss and dielectric loss (impedance mismatch loss can be ignored for $S_{11} \leq -10$ dB) for both ports. The measured realized gain is 11–12 dBi for broadside while 7–8 dBi for end-fire pattern. The discrepancy between the simulated and measured results may attribute to fabrication tolerance and the measurement errors.

4. CONCLUSION

A reconfigurable antenna printed on a single dielectric substrate with bidirectional end-fire and broadside radiation patterns has been proposed for pattern diversity applications in coal mine, crossroads, and so on. Simulations and measurements validate the performance of the proposed antenna.

ACKNOWLEDGMENTS

This work is supported by the National Basic Research Program of China under Contract 2013CB329002, in part by the National High Technology Research and Development Program of China (863 Program) under Contract 2011AA010202, and the National Natural Science Foundation of China under Contract 60771009.

REFERENCES

1. S.-H. Chen, J.-S. Row, and K.-L. Wong, Reconfigurable square-ring patch antenna with pattern diversity, IEEE Trans Antennas Propag 55 (2007), 472–475.
2. X.-S. Yang, B.-Z.Wang, W. Wu, and S. Xiao, Yagi patch antenna with dual-band and pattern reconfigurable characteristics, IEEE Antennas Wireless Propag Lett 6 (2007), 168–171.
3. T. Aboufoul, C. Parini, X. Chen, and A. Alomainy, Pattern-reconfigurable planar circular ultra-wideband monopole antenna, IEEE Trans Antennas Propag 61 (2013), 4973–4979.
4. P. Deo, A. Mehta, D. Mirshekar-Syahkal, and H. Nakano, An HIS based spiral antenna for pattern reconfigurable applications, IEEE Antennas Wireless Propag Lett 8 (2009), 196–199.
5. D. Patron, D. Piazza, and K.R. Dandekar, Wideband planar antenna with reconfigurable omnidirectional and directional radiation patterns, Electron Lett 49 (2013), 516–518.
6. J. Oh and K. Sarabandi, Compact, low profile, common aperture polarization and pattern diversity antennas, IEEE Trans Antennas Propag 62 (2014), 569–576.
7. W. Cao, B. Zhang, A. Liu, T. Yu, D. Guo, and K. Pan, A reconfigurable microstrip antenna with radiation pattern selectivity and polarization diversity, IEEE Antennas Wireless Propag Lett 11 (2012), 453–456.
8. S.L.S. Yang and K.M. Luk, Design of a wide-band L-probe patch antenna for pattern reconfiguration or diversity applications, IEEE Antennas Wireless Propag Lett 54 (2006), 433–438.
9. Y. Li, Z. Zhang, J. Zheng, Z. Feng, and M. Iskander, Experimental analysis of a wideband pattern diversity antenna with compact reconfigurable CPW-to-Slotline transition feed, IEEE Trans Antennas Propag 59 (2011), 4222–4228.
10. S.-Y. Chen, I.-C. Lan, and P. Hsu, In-line series-feed collinear slot array fed by a coplanar waveguide, IEEE Trans Antennas Propag 55 (2007), 1739–1744.
11. .Available at: http://www.ets-lindgren.com/.

A V-BAND VARIABLE GAIN AMPLIFIER WITH LOW PHASE VARIATION USING 90-nm CMOS TECHNOLOGY

Jeng-Han Tsai,[1] Jen-Wei Wang,[1] and Chung-Han Wu[2]

[1] Department of Applied Electronics Technology, National Taiwan Normal University, Taipei, Taiwan 10610, R.O.C.; Corresponding author: jhtsai@ntnu.edu.tw

[2] Graduate Institute of Communication Engineering, National Taiwan University, Taipei, Taiwan 10617, R.O.C.

Received 14 December 2013

ABSTRACT: *A V-band variable gain amplifier (VGA) with wide gain control range, low phase variation, and low return loss variation is designed and implemented on 90-nm CMOS process. Utilizing a phase compensation capacitor at the common gate transistor and a source*